Finite-size scaling analysis of isotropic-nematic phase transitions in an anisometric Lennard-Jones fluid

Manuel Greschek[1] and Martin Schoen[1,2,*]

[1]*Stranski-Laboratorium für Physikalische und Theoretische Chemie, Fakultät für Mathematik und Naturwissenschaften, Technische Universität Berlin, Straße des 17. Juni 135, D-10623 Berlin, Germany*

[2]*Department of Chemical and Biomolecular Engineering, Engineering Building I, Box 7905, North Carolina State University, 911 Partners Way, Raleigh, North Carolina 27695, USA*

(Received 15 September 2010; revised manuscript received 4 December 2010; published 21 January 2011)

By means of Monte Carlo simulations in the isothermal-isobaric ensemble, we perform a finite-size scaling analysis of the isotropic-nematic (IN) phase transition. Our model consists of egg-shaped anisometric Lennard-Jones molecules. We employ the cumulant intersection method to locate the pressure P^* at which the IN phase transition occurs at a given temperature T. In particular, we focus on second-order cumulants of the largest and middle eigenvalues of the alignment tensor. At fixed T, cumulants for various system sizes intersect at a unique pressure P^*. Various known scaling relations for these cumulants are verified numerically. At P^*, the isobaric heat capacity passes through a maximum value $c_{\mathrm{P}}^{\mathrm{m}}$, which depends on the number of molecules N. This dependency can accurately be described by a power law such that $\lim_{N\to\infty} c_{\mathrm{P}}^{\mathrm{m}}(N) \to \infty$. For sufficiently large N, the pressure at which $c_{\mathrm{P}}^{\mathrm{m}}$ is located shifts only very slightly in agreement with the apparent insensitivity of the cumulant intersection to N. In addition, we analyze our data in terms of Landau's theory of phase transitions. Our results are consistent with a weakly discontinuous entropy-driven phase transition.

DOI: 10.1103/PhysRevE.83.011704 PACS number(s): 64.70.M−, 05.10.Ln, 05.20.Jj, 64.60.an

I. INTRODUCTION

In the theory of thermal many-particle systems, today it is almost commonplace that any transition between different phases in these systems is affected by the actual size of the system under study. In fact, quite some time ago, it has been realized that thermodynamics, as the fundamental theory to treat thermal systems quantitatively, is significantly altered if it deals with small systems of finite size [1]. In statistical physics, on the other hand, conclusions are usually drawn on the basis of the explicit or implicit assumption that the so-called thermodynamic limit $N/V = \text{const}, N, V \to \infty$ (N number of molecules, V volume) exists and that it can be reached. In particular, our treatment of transformations between different phases of thermal systems often invokes the assumption of the thermodynamic limit. This poses a serious problem to the study of such phase transitions in computer simulations where one is inevitably restricted to finite systems, which typically contain less than $\sim 10^6$ particles in most practical state-of-the-art applications. In the context of discontinuous phase transitions, perhaps the most prominent signature of finite system size is the rounding of such transitions [2]. Rounding refers to the phenomenon that, in any finite system, the variation of the equilibrium-order parameter with the thermodynamic field across a phase transition can be described by a continuous curve, whereas, in an infinite system, the order parameter would change discontinuously at the onset of the phase transition (see Fig. 4.6 of Ref. [3]).

The importance of system size or, more generally, the presence of specific length scales in studies of phase transitions inspired the development of finite-size scaling concepts quite some time ago [4,5]. Generally speaking, finite-size scaling aims at a fundamental and quantitative understanding of how certain quantities computed for a finite system will change as one approaches the thermodynamic limit. Finite-size scaling, first applied to continuous phase transitions and critical phenomena, was inspired largely by renormalization group theory [6,7], a theoretical concept that first came into being in quantum electrodynamics [8]. In the meantime, overwhelming literature on the topic exists that can hardly be reviewed and summarized comprehensively in a research paper, such as the present one. Instead, for more information, the interested reader is referred to a—likely incomplete and certainly personal—selection of textbooks and review papers that have been published over the years [3,9–17].

However, to illustrate the power of finite-size scaling as a theoretical concept, it seems worthwhile to give examples of physical systems to which it has been applied successfully. Among these systems lattice models such as the Ising [4,5,18] or Potts model [19–21] rank prominently. As far as continuous model systems are concerned, finite-size scaling has been employed to investigate the gas-liquid phase transition in two- [22,23] and three-dimensional Lennard-Jones fluids [24,25]. In addition, Potoff and Panagiotopoulos also considered binary Lennard-Jones mixtures [25]. Even quantum fluids, such as the three-dimensional weakly interacting Bose gas, have been discussed within the framework of finite-size scaling [26].

In the context of this paper, finite-size scaling will be applied to the isotropic-nematic (IN) phase transition in liquid-crystalline materials. Here, finite-size scaling has been employed to obtain the critical temperature as well as various critical exponents of the planar Lebwohl-Lasher model [27]. Jayasri *et al.* used concepts of finite-size scaling within Wang-Landau Monte Carlo simulations of the three-dimensional Lebwohl-Lasher model [28]. Focusing on the IN phase transition, these authors considered the system-size dependence of the nematic order parameter S. With increasing

*martin.schoen@tu-berlin.de

lattice size, S turns out to have lower values in the isotropic phase and a steeper increase with temperature T in the immediate vicinity of the transition point. The transition itself is located via Binder's fourth-order cumulant from which it is inferred that the IN phase transition is a discontinuous one. Finite-size effects at the IN phase transition have also been investigated by Fish and Vink [29] again within the Lebwohl-Lasher model. They employ Wang-Landau Monte Carlo simulations and demonstrate that, at discontinuous IN phase transitions, the scaling is approximately that expected for a q-state Potts model. In a later publication, the same authors investigated the crossover from discontinuous to continuous IN phase transitions in confinement [30]. A careful and very detailed finite-size scaling study of the IN phase transition in nanoconfinement has been published very recently by Almarza *et al.* who based their work on the Maier-Saupe hard-sphere fluid [31]. López *et al.* used Monte Carlo simulations to study a two-dimensional lattice model of monomers that polymerize reversibly into chains [32]. Employing Binder's fourth-order cumulant, it is observed that the IN phase transition for monodisperse rods without self-assembly is of the same universality class as that of the two-dimensional Ising model; on the contrary, the model pertains to the universality class of the $q = 1$ Potts model if self-assembly is taken into account. Vink and Schilling consider the interface between isotropic and nematic phases in a system of soft spherocylinders [33]. They apply finite-size scaling concepts to obtain accurate values for the interfacial tension. However, of particular relevance to the present paper is a paper by Weber *et al.* who studied the IN phase transition in a three-dimensional bond-fluctuation lattice model of semiflexible polymers [34]. This work is of central importance for our own study because Weber *et al.* discussed, very carefully, how the IN phase transition can be located through Binder's cumulant intersection technique and, more importantly, which cumulant was most suitable for this purpose. Moreover, as we will emphasize later, their lattice model behaves qualitatively very similarly to the continuous model on which our paper is based.

In our paper, we focus on a simple model of a liquid crystal suggested originally by Hess and Su [35]. It consists of a Lennard-Jones potential in which the attractive contribution has been modified to represent the orientation-dependent interaction between slightly elongated molecules. The charm of the Hess-Su model is its simplicity. Thus, in a computer simulation, it is relatively easy to implement this model in a numerically efficient way. Despite this simplicity, the model exhibits isotropic, nematic, and smectic phases characteristic of a typical liquid crystal [36,37]. Also, the model has recently been used successfully to investigate the impact of certain anchoring scenarios at solid surfaces on the IN phase transition in nanoconfined liquid crystals [38,39]. Unfortunately, the nature of this transition is still unknown for the Hess-Su model even in the bulk. For example, the variation of the nematic-order parameter around the IN phase transition turned out to be smooth and free of hysteresis for relatively large systems of 1000–2000 molecules [36–38]. This prompted us to *speculate* [38] that, for this particular model, the IN phase transition *may perhaps* be continuous. In fact, continuous IN phase transitions are observed in two dimensions [40–42]. However, as we also emphasize in Ref. [38], a finite-size scaling analysis would be required to prove or disprove this speculation. Therefore, and in view of the usefulness of the Hess-Su model in computer simulations of both bulk and confined liquid crystals [36–39], a careful study of the mechanism of the IN phase transition seems both worthwhile and a bit overdue. Thus, the present paper is devoted to a finite-size scaling analysis of the IN phase transition in the Hess-Su model.

We have organized the remainder of this paper as follows. In Sec. II, we introduce our model system. Some basic concepts of its statistical mechanical treatment and a summary of key quantities, on which our work is based, are introduced in Sec. III. Our results are presented in Sec. IV and will be discussed further in the concluding Sec. V.

II. THE MODEL SYSTEM

We consider a bulk liquid crystal composed of N molecules interacting with each other in a pairwise additive fashion such that the configurational potential energy is given by

$$U(\boldsymbol{R},\widehat{\boldsymbol{U}}) = \frac{1}{2}\sum_{i=1}^{N}\sum_{j\neq i}^{N} u(\boldsymbol{r}_{ij},\widehat{\boldsymbol{u}}_i,\widehat{\boldsymbol{u}}_j), \tag{2.1}$$

where $\boldsymbol{r}_{ij} \equiv \boldsymbol{r}_i - \boldsymbol{r}_j$ is the distance vector between the centers of mass of particles i and j. In Eq. (2.1), $\boldsymbol{R} \equiv \{\boldsymbol{r}_1,\boldsymbol{r}_2,\ldots,\boldsymbol{r}_N\}$ and $\widehat{\boldsymbol{U}} \equiv \{\widehat{\boldsymbol{u}}_1,\widehat{\boldsymbol{u}}_2,\ldots,\widehat{\boldsymbol{u}}_N\}$ are shorthand notations for the sets of center-of-mass coordinates and unit vectors specifying the orientations of the liquid-crystalline molecules, respectively. Following earlier work [35–38], we adopt the intermolecular interaction potential,

$$u(\boldsymbol{r}_{ij},\widehat{\boldsymbol{u}}_i,\widehat{\boldsymbol{u}}_j) = 4\varepsilon\left[\left(\frac{\sigma}{r_{ij}}\right)^{12} - \left(\frac{\sigma}{r_{ij}}\right)^{6}\{1+\Psi(\widehat{\boldsymbol{r}}_{ij},\widehat{\boldsymbol{u}}_i,\widehat{\boldsymbol{u}}_j)\}\right], \tag{2.2}$$

where $r = |\boldsymbol{r}|$ and $\widehat{\boldsymbol{r}} = \boldsymbol{r}/r$. Hence, u is a Lennard-Jones potential where the attractive contribution is modified to account for different relative orientations of a pair of molecules. In Eq. (2.2), σ denotes the diameter of a spherical reference molecule, and ε is the depth of the attractive well in that reference model. The anisotropy of the fluid-fluid interaction is accounted for by the function,

$$\Psi(\widehat{\boldsymbol{r}}_{ij},\widehat{\boldsymbol{u}}_i,\widehat{\boldsymbol{u}}_j) = 5\varepsilon_1 P_2(\widehat{\boldsymbol{u}}_i\cdot\widehat{\boldsymbol{u}}_j) + 5\varepsilon_2[P_2(\widehat{\boldsymbol{u}}_i\cdot\widehat{\boldsymbol{r}}_{ij}) + P_2(\widehat{\boldsymbol{u}}_j\cdot\widehat{\boldsymbol{r}}_{ij})], \tag{2.3}$$

which one obtains from a summation of certain Wigner matrices selected to preserve the head-tail symmetry of the molecules [35]. In other words, Ψ remains unaltered if $\widehat{\boldsymbol{u}}_i$ and/or $\widehat{\boldsymbol{u}}_j$ are replaced by $-\widehat{\boldsymbol{u}}_i$ and/or $-\widehat{\boldsymbol{u}}_j$. As in our previous paper, we take $\varepsilon_1 = 0.04$ and $\varepsilon_2 = -0.08$ for the anisotropy parameters such that the aspect ratio of each molecule is $\sim$1.26 (see Fig. 1) [38]. In Eq. (2.3),

$$P_2(x) = \tfrac{1}{2}(3x^2-1) \tag{2.4}$$

is the second Legendre polynomial.

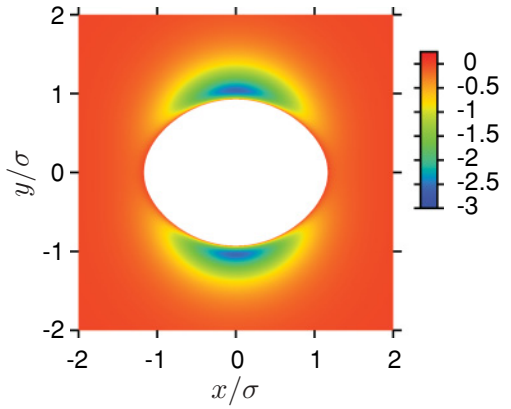

FIG. 1. (Color online) Plots of $u(\boldsymbol{r}_{12},\widehat{\boldsymbol{u}}_1,\widehat{\boldsymbol{u}}_2)$ for a pair of molecules located in the x-y plane such that $\boldsymbol{r}_{12}=(x_{12},y_{12},0)$ and $\widehat{\boldsymbol{u}}_1\cdot\widehat{\boldsymbol{u}}_2=1$. The white area at the center of the plot is defined by the condition $u_{\rm ff}(\boldsymbol{r}_{12},\widehat{\boldsymbol{u}}_1,\widehat{\boldsymbol{u}}_2)\geqslant 0$ such that it approximately represents the shape of the molecule at the center of the coordinate system true to scale. In colored parts of the figure, $u_{\rm ff}(\boldsymbol{r}_{12},\widehat{\boldsymbol{u}}_1,\widehat{\boldsymbol{u}}_2)<0$ where the color (see attached color bar) indicates the local value $u_{\rm ff}$ of in units of ε.

III. THEORETICAL BACKGROUND

A. Statistical thermodynamics

For reasons to be explained later (see Sec. IV A), we choose to describe the thermodynamic state of the liquid crystal in terms of N, temperature T, and pressure P as natural variables. This immediately suggests the Gibbs potential $\mathcal{G}$ as the relevant thermodynamic potential, which assumes a minimum at equilibrium. One of the quantities we are interested in is the isobaric heat capacity, which can be derived from the exact differential of $\mathcal{G}$ via

$$\frac{c'_{\rm P}}{T}\equiv\left(\frac{\partial\mathcal{S}}{\partial T}\right)_{\{\cdot\}\backslash T}=-\left(\frac{\partial^2\mathcal{G}}{\partial T^2}\right)_{\{\cdot\}\backslash T}, \tag{3.1}$$

where $\mathcal{S}$ denotes entropy and $\{\cdot\}\backslash x$ is a shorthand notation to indicate that, upon differentiation, the set of natural variables of $\mathcal{G}$ is to be held constant except for variable x. In this paper, we consider the *specific* heat capacity $c_{\rm P}=c'_{\rm P}/N$.

The connection to a molecular level of description is provided through another textbook expression (see, for example, Chap. 3.29 of Ref. [43]), namely,

$$\mathcal{G}=-k_BT\ln\chi\,(N,P,T)\,, \tag{3.2}$$

where k_B is the Boltzmann constant,

$$\chi=\sum_V\exp\left(-\beta PV\right)\mathcal{Q}\,(N,V,T) \tag{3.3}$$

is the partition function in the isothermal-isobaric ensemble, V denotes volume, and $\beta\equiv 1/k_BT$. In Eq. (3.3), $\mathcal{Q}$ is the canonical ensemble partition function in the classical limit. As explained for arbitrary molecular symmetry in the book by Gray and Gubbins [44] and later for the special case of linear molecules by Gruhn and Schoen [45], one may express $\mathcal{Q}$ as

$$\mathcal{Q}=\frac{1}{\Lambda^{5N}}\left(\frac{I}{m}\right)^N\mathcal{Z}, \tag{3.4}$$

where

$$\mathcal{Z}=\frac{1}{2^N N!}\int d\boldsymbol{R}d\widehat{\boldsymbol{U}}\exp(-\beta U) \tag{3.5}$$

is the configuration integral. In Eq. (3.4), $\Lambda\equiv h/\sqrt{2\pi mk_BT}$ is the thermal de Broglie wavelength (h is the Planck constant), and m and I denote molecular mass and moment of inertia, respectively. The factor $1/2^N$ in Eq. (3.5) corrects for double counting equivalent configurations characterized by $\widehat{\boldsymbol{u}}_i$ and $-\widehat{\boldsymbol{u}}_i$ (head-tail symmetry).

B. Properties

From quantities introduced in Sec. III A, we can derive molecular expressions for $c_{\rm P}$. Details of this derivation can be found elsewhere [38]. After considerable but straightforward algebra, one eventually obtains

$$c_{\rm P}=\frac{5}{2}k_B+\frac{\langle\mathcal{H}^2\rangle-\langle\mathcal{H}\rangle^2}{Nk_BT^2}, \tag{3.6}$$

where $\langle\cdots\rangle$ denotes an ensemble average in the isothermal-isobaric ensemble. In Eq. (3.6), the energy function $\mathcal{H}\equiv U(\boldsymbol{R},\widehat{\boldsymbol{U}})+PV$ such that $\frac{5}{2}k_BT+\langle\mathcal{H}\rangle$ can be interpreted as the enthalpy of the liquid crystal. At a phase transition, $c_{\rm P}$ undergoes a characteristic change [46] and, therefore, is a useful quantity in the context of this paper.

Moreover, the IN phase transition is characterized by a change in orientational order. To determine the degree of orientational order, we follow Maier and Saupe and introduce the nematic-order parameter S [47,48] (see also Refs. [49,50]). This order parameter is defined such that $S=0$ in an infinitely large isotropic phase, whereas $S\simeq 1$ if the symmetry axes of all molecules point in the direction of the unit vector $\widehat{\boldsymbol{n}}$ usually referred to as the director. Because $\widehat{\boldsymbol{n}}$ is *a priori* unknown, a derivation of a molecular expression for S conveniently departs from the so-called alignment tensor [51],

$$\mathbf{Q}\equiv\frac{1}{2N}\sum_{i=1}^{N}(3\widehat{\boldsymbol{u}}_i\otimes\widehat{\boldsymbol{u}}_i-\mathbf{1})\,, \tag{3.7}$$

where $\otimes$ denotes the direct (i.e., dyadic) product and $\mathbf{1}$ is the unit tensor. The alignment tensor can be represented by a real symmetric traceless 3×3 matrix that can be diagonalized numerically using Jacobi's method (see, for example, Chap. 11.1 of Ref. [52]). This procedure allows one to compute the three eigenvalues $\lambda_-<\lambda_0<\lambda_+$ of $\mathbf{Q}$ and the associated eigenvectors. Following previous workers [34,38,53,54], we define the nematic-order parameter through the expression $S\equiv\langle\lambda_+\rangle$ and take, as $\widehat{\boldsymbol{n}}$, the eigenvector associated with the largest *instantaneous* eigenvalue λ_+. Hence, $\widehat{\boldsymbol{n}}$ may vary during the course of the simulation. Moreover, a basic theorem of linear algebra establishes the trace of a tensor as one of its scalar invariants (see, for example, Chap. 4.2 of Ref. [55]). Therefore, $\mathrm{Tr}\,\mathbf{Q}=\mathrm{Tr}\,(\mathrm{diag}\,\mathbf{Q})=0$ where the operator Tr represents the trace and

$$\mathrm{diag}\,\mathbf{Q}\equiv\begin{pmatrix}-\lambda_+/2-\zeta & 0 & 0\\ 0 & -\lambda_+/2+\zeta & 0\\ 0 & 0 & \lambda_+\end{pmatrix}, \tag{3.8}$$

in the basis of eigenvectors of **Q**. In Eq. (3.8), ζ may be taken as a measure of apparent biaxiality. This expression was derived by Low who uses an expansion in terms of Wigner matrices [56]. As already pointed out by Eppenga and Frenkel [54], ζ is nonzero in any finite system even in the isotropic phase (see also Sec. IV B). Because such finite-size effects are the focus of the present paper, it is useful to introduce the ostensible biaxiality-order parameter $\xi \equiv \langle \zeta \rangle$ in accord with the definition of S introduced before.

In the study of finite-size effects at phase transitions, order-parameter *distributions* and their moments have been established as powerful tools [3]. In particular, suitably defined *ratios* of these moments known as cumulants are particularly useful [4,5]. For a nonvanishing order parameter $\langle O \rangle$, the nth-order cumulant may be defined as

$$g_n \equiv \frac{\langle O^n \rangle}{\langle O \rangle^n}, \tag{3.9}$$

where

$$\langle O^n \rangle = \int_0^1 d\widetilde{O}\, \widetilde{O}^n \mathcal{P}(\widetilde{O}), \tag{3.10}$$

and $\mathcal{P}(O)$ is the order-parameter distribution, which can be computed as a histogram of O in a computer simulation. In many applications, g_4 has been considered (see, for example, Refs. [3,12]). However, from the definition of g_n in Eq. (3.9) and the expression in Eq. (3.10), it is apparent that the wings of $\mathcal{P}(O)$ are probed more the larger n becomes. Unfortunately, the accuracy of numerically determined histograms $\mathcal{P}(O)$ decreases rapidly as one moves into these wings where $\mathcal{P}(\widetilde{O}) \to 0$. To circumvent this problem, Weber *et al.* proposed to employ lower-order cumulants, such as g_2 [34]. We follow this proposition in Sec. IV C and, in particular, investigate g_2 for $O = -\lambda_0 = -\lambda_+/2 + \zeta$ and $O = \lambda_+$ as the relevant order parameters.

It has also been argued by Weber *et al.* [34] that, at a continuous phase transition,

$$\langle O^n(\cdot, L) \rangle = L^{n\beta/\nu} \mathcal{X}(\cdot, L/\ell), \tag{3.11}$$

where L is the linear dimension of the system, β is the order-parameter critical exponent, ν is the critical exponent governing the divergence of the correlation length ℓ at the critical point, and $\mathcal{X}$ is a scaling function depending on the thermodynamic field driving the phase transition (represented by $\cdot$) and on the ratio L/ℓ. Directly at the critical point, $\ell \to \infty$. Hence, in computing g_n directly at the critical point causes curves for different L to intersect in a single nonuniversal (i.e., model-dependent) point [3,20]. If, on the other hand, the phase transition is discontinuous but rounded on account of the finite size of the system under study, g_n for different L do not have to intersect in a single point. Specifically, a pair of curves for different L may intersect such that the relative magnitude of g_n for any two system sizes reverses at the location of the phase transition. The intersection may still be system-size dependent and may then scale as L^{-d} ($N^{-d/3}$) where d is the dimension of the system as shown by Vollmayr *et al.* for the q-state Potts model [20]. This prediction was confirmed later by Weber *et al.* for their lattice model of flexible polymers [34]. However, it seems worthwhile to note at this point that the shift of the cumulant intersection may already be very weak over a range of (sufficiently large) system sizes and, therefore, hard, if not impossible, to detect, although the phase transition is truly discontinuous.

For a discussion of the nature of the IN transition (i.e., whether it constitutes a continuous or a discontinuous phase transition for the present model), it will turn out to be prudent to determine the correlation length ℓ of orientational correlations. To that end, it is useful to introduce the orientation correlation function,

$$G_2(r) = \langle P_2[\cos\alpha(r)] \rangle, \tag{3.12}$$

where $\cos\alpha(r) = \widehat{\boldsymbol{u}}_1(\boldsymbol{r}_1) \cdot \widehat{\boldsymbol{u}}_2(\boldsymbol{r}_2)$ is the cosine of the angle $\alpha(r)$ formed between the molecular directors $\widehat{\boldsymbol{u}}_1$ and $\widehat{\boldsymbol{u}}_2$ of a pair of molecules separated by a distance $r = |\boldsymbol{r}_1 - \boldsymbol{r}_2|$ (see, for example, Ref. [57]). The subsequent discussion will particularly benefit from introducing the so-called *connected* correlation function,

$$G_2^{\mathrm{c}}(r) \equiv G_2(r) - S^2 \xrightarrow{r\to\infty} 0. \tag{3.13}$$

Assuming an exponential decay of $G_2(r)$ in a sufficiently large system [27,58], one may obtain a quantitative estimate of ℓ by fitting $f(r) = a\exp(-r/\ell)$ to $G_2^{\mathrm{c}}(r)$ in the limit of sufficiently large r taking a and ℓ as fit parameters.

IV. RESULTS

A. Numerical aspects

To compute the quantities introduced in Sec. III B, we employ Monte Carlo simulations in the isothermal-isobaric ensemble in which a fluid composed of a fixed number of molecules N is exposed to a pressure P that remains constant during the course of an individual simulation. Consequently, the volume V of the simulation cell may fluctuate. We employ periodic boundary conditions in all three spatial directions. To generate a Markov chain of configurations in this ensemble, we utilize the algorithm described in Sec. 4.1 of Ref. [59]. As part of this algorithm attempts to change the volume of the simulation, cells have to be incorporated properly. In the simulation of ordered (nematic or smectic) phases of anisometric molecules, one would normally want to change the lengths of the simulation cell independently in each spatial direction such that these ordered phases can be accommodated properly. This is particularly important in the formation of smectic phases of molecules with a large aspect ratio. If, for example, the length of the simulation cell in the direction of the smectic layers would not be close to an integer multiple of the thickness of a smectic layer, the entire fluid would be under an artificial and unphysical stress because the smectic phase could not fit properly into the simulation cell. For the present model in which the molecules have a rather small aspect ratio of $\sim$1.26 and because we are not interested in smectic phases, this problem does not arise. We have verified this by monitoring diagonal components of the pressure tensor $\mathbf{P} = P\mathbf{1}$ separately during the course of the simulation [38]. Thus, we assume our simulation cell to be roughly cubic throughout this paper and change the volume of the simulation cell isotropically, that is, simultaneously and by the same small amount δ_{s} in each spatial direction. We adjust δ_{s}, which is typically of the order of only a few percent of σ [see Eq. (2.2)], during the course

of a simulation to achieve an acceptance ratio of 40%–60% of all attempted changes of simulation-cell volume.

We refer to a Monte Carlo cycle as a sequence of N attempted displacements or rotations of sequentially selected fluid particles plus one attempted change of V. Rotations and displacements are attempted with equal probability. Most runs comprise initial 5×10^4 Monte Carlo cycles for equilibration followed by 2×10^5 Monte Carlo cycles; for the largest systems with $N = 5000$ and 10 000, and, in the immediate vicinity of such a transformation, the length of a typical run was enlarged up to 4×10^5 Monte Carlo cycles to guarantee sufficient statistical accuracy.

We express all quantities of interest in terms of the customary dimensionless (i.e., reduced) units. For example, length is given in units of σ, energy in units of ε, and temperature in units of ε/k_B. Other derived quantities are expressed in terms of suitable combinations of these basic quantities. For example, pressure is given in units of ε/σ^3. Throughout this paper, we fix the temperature $T = 1.0$, which should be sufficiently low to allow for a formation of both isotropic and nematic phases where we take the mean-field bulk phase diagram of Hess and Su as a rough guidance [35]. To save computer time, we cut off fluid-fluid interactions beyond a separation of $r_c = 3.0$ between the centers of mass of a pair of fluid molecules with no shift [31] or long-range correction applied. In addition, we employ a combination of a linked-cell and a conventional (Verlet) neighbor list as described in the book by Allen and Tildesley to further speed up the simulations (see Chap. 5.3 of Ref. [60]). This latter list includes all particles as neighbors whose centers of mass are located within a distance of $r_n = 3.5$ from a reference molecule at the origin of the neighbor sphere. Under these conditions, the smallest system we can study comprises $N = 250$ molecules. If $N < 250$, the actual side lengths of the simulation cell could become shorter than $2r_c$ such that the minimum image convention [60] would be violated. We could accommodate these smaller systems if we reduce r_c. However, this would inevitably change the physical nature of our model fluid. A comparison with our earlier papers [38,39] would then be disabled. Consequently, the simulations presented in this paper have been carried out for systems containing $250 \leqslant N \leqslant 5000$ molecules. A few simulations for $N = 10\,000$ have also been included to check certain scaling laws. However, these simulations take approximately up to 4 days of CPU time per state point on our computer cluster and, therefore, are too time consuming to be carried out routinely.

Finally, a comment seems appropriate concerning the choice of the isothermal-isobaric ensemble for this paper. Ideally, one would prefer to study phase transitions in the grand canonical ensemble [61]. Unfortunately, the IN phase transition normally arises in a density regime where the Metropolis algorithm adapted to simulations in the grand canonical ensemble is rather inefficient or breaks down completely [60]. The reason is that, during the particle creation or deletion substep of the adapted Metropolis algorithm, it becomes increasingly difficult to either remove existing particles mostly located at energetically favorable positions or to create new ones at energetically favorable holes as the fluid's average density increases. Because N is fixed in isothermal-isobaric Monte Carlo simulations, this problem does not arise so that this latter ensemble seems a better choice for the present paper. However, it is noteworthy that finite-size scaling procedures developed originally for the grand canonical ensemble may be transferred to the isothermal-isobaric ensemble without modification as shown by Wilding and Binder a while ago [61].

B. Finite-size effects

In the context of the IN phase transition, finite-size effects manifest themselves most notably in the nematic-order parameter S introduced in Sec. III B. As one can see from plots in Fig. 2(a), S does not vanish at low pressures in the isotropic phase but remains nonzero. Generally speaking, S increases with P as one goes from the isotropic ($P = 1.0$) to the nematic phase ($P = 2.0$). Our data show that S, in the isotropic phase, is larger the smaller N is. In going from the isotropic to the nematic phase, the overall increase of S with P is smaller the smaller N is. Around the IN phase transition, S increases more steeply as the number of molecules in the system becomes larger. On the contrary, the dependence of S on N in the nematic phase is much smaller. These features, which are relatively easy to understand, already have been reported and have been discussed many times in the literature. They are observed in quite different model systems, such as hard platelets [54], lattice polymers of variable stiffness [34], polydisperse mixtures of soft spherocylinders [53], and even under nanoconfinement conditions [31].

In a typical liquid-crystalline material, the interaction between a pair of mesogens is such that a parallel orientation of both members of the pair is usually favored regardless of whether these interactions are purely entropic or of a van der Waals type. In general, these interactions have a small but nonvanishing range so that the preferred relative orientation of a pair of nearest neighbors is transferred, to some extent, to more distant molecules. Hence, at the molecular level, nanoscopic clusters form in which molecules exhibit nematic order, although the thermodynamic state of the entire liquid crystal pertains to the isotropic phase. On account of thermal fluctuations, sufficiently remote clusters may have local directors pointing in different and uncorrelated directions. In an infinite system, where one would average over a vast (i.e., essentially infinite) number of such clusters, the order parameter would vanish identically according to its definition. In a finite system, however, and no matter how big the system is, some residual order inevitably remains, and this is the reason for the nonvanishing values of S in the isotropic phase that become smaller as N increases as one can see from Fig. 2(a).

The finite-size effect also manifests itself as an ostensible biaxiality as can be seen from plots in Fig. 2(b). In an infinite system and according to its definition, ξ should vanish in the isotropic phase where no preferred orientation of the molecules exists. It should also vanish in a perfect nematic phase of uniaxial symmetry. On the contrary, plots of ξ versus P in Fig. 2(b) reveal that, even in the isotropic phase, a substantial biaxiality exists that becomes smaller with increasing N. As one moves into the nematic regime, ξ becomes smaller because of the increasing uniaxiality of these phases where $\hat{\boldsymbol{n}}$ represents the dominant symmetry axis. Our results show that this drop of ξ may be relatively sharp in large systems (e.g., $N = 5000$),

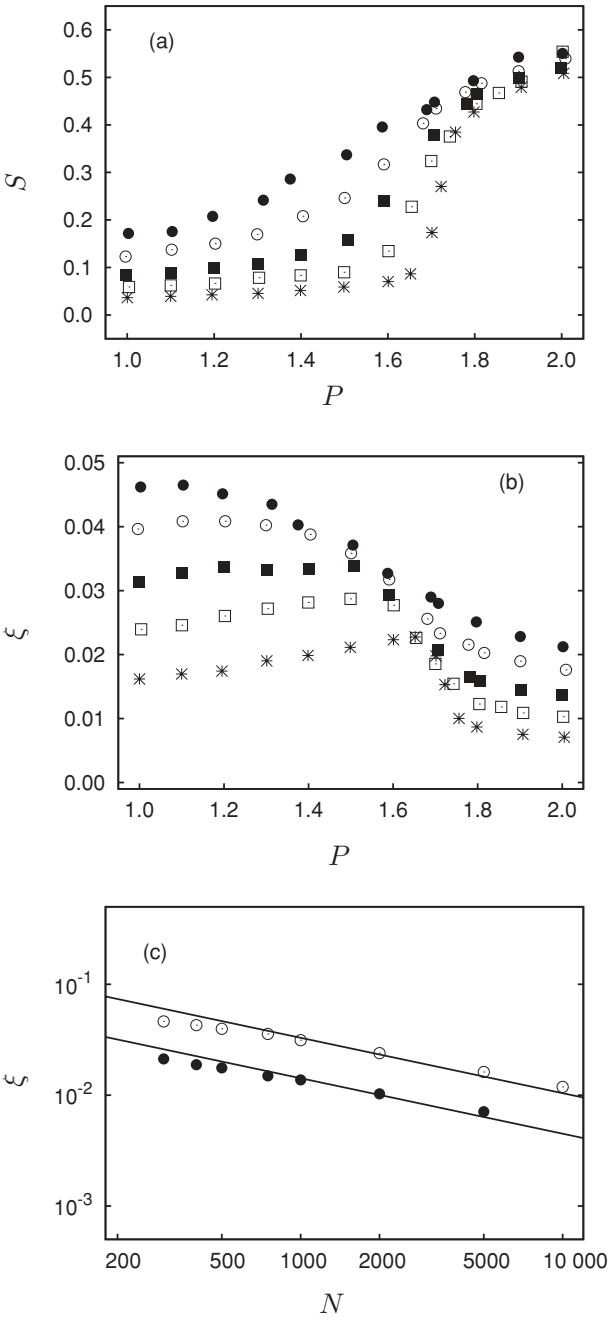

FIG. 2. (a) Nematic-order parameter S as function of applied pressure P; ●, $N = 300$; ○, $N = 500$; ■, $N = 1000$; □, $N = 2000$; and ∗, $N = 5000$. (b) as (a) but for the biaxial order parameter ξ. (c) ξ as a function of N for ○, $P = 1.0$ in the isotropic and ●, $P = 2.0$ in the nematic phases; solid lines are fits of $aN^{-1/2}$ to the discrete data points where ○, $a = 1.042$ and ●, $a = 0.449$, respectively (see Sec. IV C).

whereas, in smaller systems (e.g., $N = 300$), the variation of ξ with P is much weaker around the IN phase transition. Nevertheless, a small residual ostensible biaxiality remains even for the largest system and deep in the nematic phase as the plot of ξ for $N = 5000$ molecules and $P = 2.0$ in Fig. 2(b) shows. Moreover, the plot in Fig. 2(c) shows that our data can be very well represented by a power law providing further support for the presence of a perhaps vanishingly small but always nonzero residual ostensible biaxiality in the nematic phase of any finite system. The power law decay of ξ will be rationalized later in Sec. IV C.

C. Cumulant analysis

Because of the finite-size effects demonstrated in Sec. IV B, it is not immediately obvious at which pressure P the IN phase transition occurs in the thermodynamic limit nor what the nature (i.e., continuous versus discontinuous) of this phase transition is for the present model. For example, as Fig. 2(a) already indicated, the variation of S around the (assumed) phase transition becomes steeper with increasing N but still looks rather continuous, which would point toward a continuous phase transition. However, one knows that, in any finite system, phase transitions appear to be more or less rounded depending on the specific phase transition and the actual system size [3]. Hence, for the present model, even the system comprising $N = 5000$ molecules may still be too small to reveal the true discontinuous steplike change of S at a discontinuous IN transition on account of the relative weakness of the transition. The notion that the IN phase transition in the Hess-Su model may be unusually weak is further corroborated by the surprisingly small increase of S across that transition. For example, it is evident from plots in Fig. 2(a) that S does not exceed 0.6 even deep in the nematic regime. This value is less than $\frac{2}{3}$ of the ideal value $S = 1$ in a nematic phase in which nearly all molecules are perfectly aligned with $\hat{\boldsymbol{n}}$ [62]. Further evidence for the formation of only weakly ordered nematic phases in the Hess-Su model is provided by the observation that, in our Monte Carlo simulations, the angle increment for the random orientation of molecules is adjusted to a remarkably large value of $\Delta\alpha \simeq \frac{\pi}{2}$ to preserve an acceptance ratio of roughly 0.5 even deep in the nematic phase at $P \simeq 2.0$. This shows that, after the nematic phase has formed, molecules are still relatively free to rotate, thus, explaining the small values of S and, perhaps, the weakness of the IN phase transition in the Hess-Su model. Consequently, the apparent smoothness of the curves in Fig. 2(a) may erroneously be misinterpreted as a signature of a continuous IN phase transition.

To locate the transition point and to shed more light on the nature of the IN phase transition, it has been demonstrated, quite some time ago, in the pioneering work by Binder [3–5] that cumulants of suitably chosen order parameters are very useful not only in locating the transition point, but also in determining the nature of a specific phase transition. In this paper, we focus on the second-order cumulants g_2^0 and g_2^+ following the suggestion of Weber *et al.* [34], where the superscript refers to the associated eigenvalues λ_0 and λ_+ of $\mathbf{Q}$, respectively. Before turning to a detailed analysis of both cumulants and in view of a similar analysis performed earlier by Weber *et al.* for a lattice model of flexible polymers [34], it seems worthwhile to investigate the scaling behavior of those moments of λ_0 and λ_+ on which both cumulants are based [see Eq. (3.9)]. In the isotropic phase, one anticipates

$$\langle\lambda_0\rangle \propto N^{-1}, \tag{4.1a}$$

$$\langle\lambda_0^n\rangle \propto N^{-n/2}, \quad n \geqslant 2, \tag{4.1b}$$

$$\langle\lambda_+^n\rangle \propto N^{-n/2}. \tag{4.1c}$$

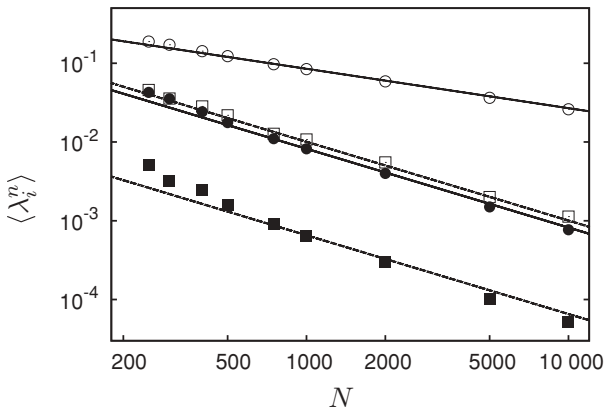

FIG. 3. Moments of the order-parameter distribution $\mathcal{P}(\lambda_i)$ ($i = 0,+$) [see Eq. (3.10)] as functions of N for $P = 1.0$ in the isotropic phase. Results are shown for ○, $i = +$, $n = 1$; ●, $i = +$, $n = 2$; □, $i = 0$, $n = 1$; and ■, $i = 0$, $n = 2$. Solid and dashed lines represent the various scaling laws given in Eqs. (4.1) (see text).

The scaling laws given in Eqs. (4.1a) and (4.1c) for $n = 1$ have been obtained analytically by Eppenga and Frenkel [54], whereas the ones given in Eqs. (4.1b) and (4.1c) have been conjectured and numerically confirmed by Weber *et al.* [34].

Plots in Fig. 3 confirm the scaling laws introduced in Eq. (4.1) quite nicely for a range of particle numbers varying by a factor of 40 between the smallest and the largest one considered. In terms of an associated variation of the side length of the (cubic) simulation cell, this translates to a, perhaps, somewhat less impressive factor of only 3.4 if this number is compared with a factor of 32 by which Weber *et al.* have varied the number of lattice sites in one spatial dimension [34]. However, one has to keep in mind that these latter authors employed a (three-dimensional) lattice model, which—like most, if not all lattice models—is computationally much less demanding than a continuous model, such as the one studied here. Nevertheless, it is gratifying that even over a smaller range of system sizes, our data already obey the asymptotic behavior predicted by Eqs. (4.1). We have made this test as rigorous as possible by fitting power laws aN^{-b} to the discrete Monte Carlo data where we only took a but not b as a fit parameter; values for b are taken directly from Eqs. (4.1). This procedure also enables us to detect a small deviation from the scaling laws as far as $\langle \lambda_0 \rangle$ and $\langle \lambda_0^2 \rangle$ for $N < 500$ are concerned. This deviation from the scaling laws indicates that these systems may be a little bit too small for the asymptotic expressions in Eqs. (4.1) to be fully valid. In fact, for insufficiently large N, there should be correction terms to the asymptotic expressions given in Eqs. (4.1) (see, for example, Eqs. (A12) of Ref. [54]).

Also, we are now in a position to rationalize the scaling behavior of the ostensible biaxiality already displayed in Fig. 2(c). From Eq. (3.8), it follows that

$$\xi \equiv \langle \zeta \rangle = \langle \lambda_+ \rangle \left(\frac{1}{2} + \frac{\langle \lambda_0 \rangle}{\langle \lambda_+ \rangle} \right) \overset{N \to \infty}{\propto} N^{-1/2}, \tag{4.2}$$

where we employed the scaling laws stated in Eqs. (4.1). In the nematic phase, however, Eppenga and Frenkel's analysis indicates a different scaling behavior of the eigenvalues of $\mathbf{Q}$, namely,

$$\langle \lambda_0 \rangle \propto N^{-1/2}, \tag{4.3a}$$

$$\langle \lambda_+ \rangle \propto N^{-1}, \tag{4.3b}$$

such that

$$\xi = \langle \lambda_0 \rangle \left(\frac{1}{2} \frac{\langle \lambda_+ \rangle}{\langle \lambda_0 \rangle} + 1 \right) \overset{N \to \infty}{\propto} N^{-1/2} \tag{4.4}$$

leads to the same scaling behavior of the ostensible biaxiality in both isotropic and nematic phases. Our data plotted in Fig. 2(c) are consistent with both Eqs. (4.2) and (4.4) as far as sufficiently large systems ($N \gtrsim 500$) are concerned. Deviations from the scaling laws in Eqs. (4.2) and (4.4) at smaller particle numbers are anticipated on account of additional N-dependent corrections that were neglected in our analysis [54]. However, our data do not permit us to verify Eqs. (4.3) directly because, in the nematic phase, the variation of both eigenvalues over the range of system sizes considered is vanishingly small as one can see, for instance, from the plots in Fig. 2(a).

After analyzing these various scaling laws, it follows from Eqs. (4.1) and the plots in Fig. 3 that, in the isotropic phase, $g_2^+ \approx c$ and $g_2^0 \propto N$ where c is a nonuniversal model-specific constant. This scaling behavior of the cumulants makes it somewhat more cumbersome to analyze g_2^+ because curves for different N bundle up in the isotropic phase as we will demonstrate shortly. A similar bundling up is not expected for g_2^0, and this is the reason why analyzing this latter cumulant was suggested earlier by Weber *et al.* [34]. However, we will show later that both cumulants provide data sets that are consistent with each other. However, before turning to that discussion, it seems worthwhile to point out that numerical accuracy of g_2^0 in the isotropic phase decreases with increasing N despite the more favorable scaling behavior. This is because an increasing value of g_2^0 with increasing N is obtained by taking the ratio of two numbers, both of which tend to zero as $N \to \infty$ [see Eqs. (3.9), (4.1a), and (4.1b)]. Therefore, the accuracy of g_2^0 is expected to go down with system size. Focusing on small systems to circumvent this problem is not advisable either because the linear dimension(s) of the simulation cell may eventually become comparable in magnitude with ℓ. In this latter case, one has to be prepared for additional features that render the interpretation of the cumulant difficult [34].

Plots in Fig. 4(a) illustrate the behavior of g_2^+ with P and for different system sizes. In the isotropic regime, one clearly sees the bundling up of curves for different N as anticipated. As P increases, g_2^+ decreases monotonically as far as smaller systems ($N \leqslant 500$) are concerned. In larger systems, g_2^+ exhibits a nonmonotonic dependence on P and passes through a maximum located at a system-size-dependent pressure in the isotropic phase [cf., Fig. 2(a)]. The height of this maximum, which is most clearly visible in the plot for $N = 5000$, increases with N similar to what has been observed earlier by Weber *et al.* [34]. Most importantly, however, curves for different N have a common intersection at the transition pressure $P^* \simeq 1.74$ and reverse their magnitude for $P > P^*$. Comparing Figs. 4(a) and 4(b), one notices a

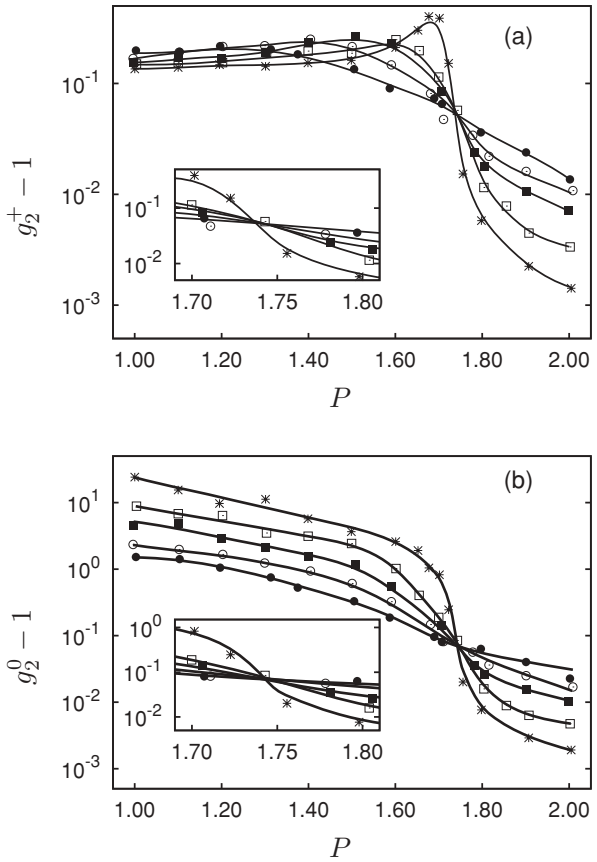

FIG. 4. (a) Second-order cumulant $g_2^+ - 1$ as a function of applied pressure P; ●, $N = 300$; ○, $N = 500$; ■, $N = 1000$; □, $N = 2000$; and ∗, $N = 5000$. (b) as (a) but for g_2^0. The insets show enlargement of plots around the IN phase transition (see text).

couple of differences. First, as predicted on the basis of Eqs. (4.1a), (4.1b), and Fig. 3, plots of g_2^0 in Fig. 4(b) do not bundle up in the isotropic phase. In fact, g_2^0 at $P = 1.0$ changes by little more than an order of magnitude over the range $300 \leqslant N \leqslant 5000$ as expected. The pressure dependence of all curves is monotonic. All curves intersect at $P^* \simeq 1.74$ (as do the curves g_2^+), where they change their curvature and reverse their order for $P > P^*$. Hence, from plots in both parts of Fig. 4, we conclude that the IN phase transition at $T = 1.0$ occurs at $P_{\mathrm{IN}} = P^* \simeq 1.74$.

D. Nature of the isotropic-nematic phase transition

Although this result and the observation of a common cumulant intersection for both g_2^+ and g_2^0 are gratifying, they still leave the question concerning the *nature* of the IN phase transition unanswered. For example, the fact that a common intersection of the second-order cumulants exists is not necessarily indicative of a continuous phase transition as emphasized earlier by Vollmayr *et al.* [20]. On the contrary, a unique cumulant intersection could also mean that the system-size-dependent shift of the intersection characteristic of a discontinuous phase transition is too weak to be detected over the range of system sizes accessible and the statistical accuracy with which g_2^+ and g_2^0 can be computed.

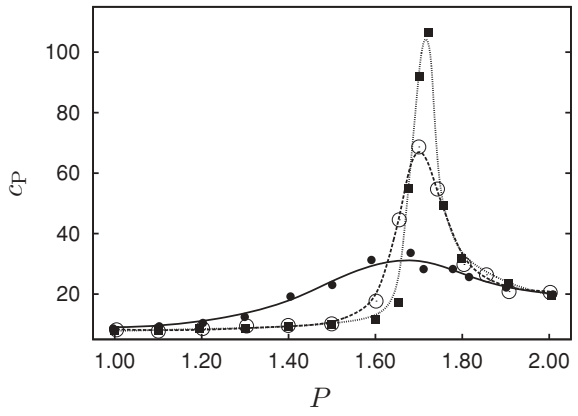

FIG. 5. Isobaric heat capacity c_{P} as a function of applied pressure P; ●, $N = 300$; ○, $N = 2000$; and ■, $N = 5000$.

To gain more insight into the nature of the IN phase transition, we considered additional quantities in this paper. Plots in Fig. 5 show the variation of the isobaric heat capacity [see Eq. (3.6)] as a function of pressure for three selected system sizes. One notices that sufficiently far away from the maximum, the heat capacity apparently is independent of N. This holds for low pressures in the isotropic as well as for sufficiently high pressures in the nematic phases. In the vicinity of the phase transition, the shape of c_{P} exhibits a marked system-size dependence. Generally speaking, the larger N, the sharper and taller the maximum $c_{\mathrm{P}}^{\mathrm{m}}$ of the curve c_{P}. For the largest system of $N = 5000$ molecules considered in Fig. 5, the location of $c_{\mathrm{P}}^{\mathrm{m}}$ agrees very well with $P^* \simeq 1.74$ obtained via the cumulant intersection approach and, therefore, is taken as a fingerprint of the IN phase transition as in our previous work [38,39]. One also sees from Fig. 5 that the location of $c_{\mathrm{P}}^{\mathrm{m}}$ is remarkably insensitive to the system size, whereas, both the width of the curves plotted in Fig. 5 as well as the height of their maximum depend strongly on N.

According to Vollmayr *et al.*, one expects $c_{\mathrm{P}}^{\mathrm{m}}$ in a three-dimensional system to scale with $N^{2/3\nu-1}$ if the IN phase transition is continuous [20]. In this scaling relation, $\nu = 0.6289$ is the relevant critical exponent [63] such that the divergence of $c_{\mathrm{P}}^{\mathrm{m}}$ with increasing system size at a continuous phase transition would be rather weak. If, on the other hand, the IN phase transition was discontinuous, $c_{\mathrm{P}}^{\mathrm{m}}$ should increase linearly with N [20]. However, in analyzing the scaling behavior of $c_{\mathrm{P}}^{\mathrm{m}}$, some care has to be taken. This is because it was pointed out by Bruce and Wilding [64] and reemphasized more recently by Fernandez *et al.* [65] that the scaling law for $c_{\mathrm{P}}^{\mathrm{m}}$ contains an analytical background that does not scale with system size (see, for example, Eq. (48) of Ref. [65]). As we show in Fig. 6, $c_{\mathrm{P}}^{\mathrm{m}}$ may be represented by an expression of the form $aN^y + b$. Fitting this expression to our data, the analytic background $b \simeq 8.2$ turns out to be rather substantial and amounts to roughly $\frac{1}{4}$ of $c_{\mathrm{P}}^{\mathrm{m}}$ for $N = 300$. In addition, our fit gives $y \simeq 0.58$, which is much larger than the value $2/3\nu - 1 \simeq 0.06$ expected for a continuous phase transition. Nevertheless, our value of y is still smaller than 1, which would be anticipated for a strongly discontinuous IN transition. A scaling behavior intermediate between those characteristics of a continuous and that of a discontinuous phase transition

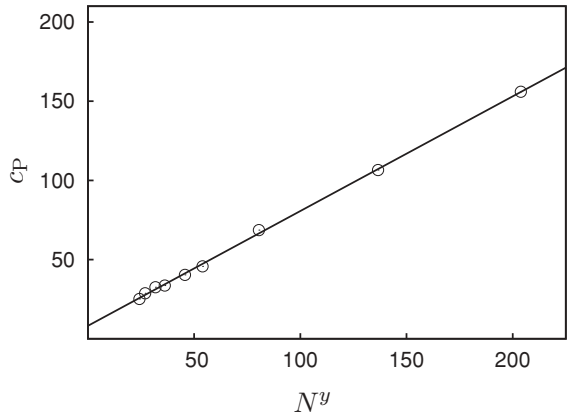

FIG. 6. Maximum of the isobaric heat capacity c_P^m as a function of the number of molecules N^y where $y \simeq 0.58$ is obtained by fitting the expression $aN^y + b$ to the simulation data.

has been reported earlier by Vollmayr *et al.* for the q-state Potts model [20]. However, Vollmayr *et al.* did not include the analytical background in their scaling analysis of c_P^m. Nevertheless, we follow these authors and conclude that, for the Hess-Su model, the IN phase transition is most likely to be weakly discontinuous because our value of y turns out to be midway between that characteristic of a continuous and that of a strongly discontinuous phase transition.

Further evidence for this conclusion is provided by an inspection of the orientational correlation function $G_2(r)$ [see Eq. (3.12)] plotted in Fig. 7 for two state points in the immediate vicinity of the IN phase transition at $P \simeq 1.735$ and 1.745. These values are very close to $P^* \simeq 1.74$ at which all cumulants g_2^0 and g_2^+ intersect (see Fig. 4). For a large system containing $N = 10\,000$ molecules, both curves converge nicely to their asymptotic values S^2 within the range of accessible intermolecular distances. For the state at lower pressure $P = 1.735$, the system is still in its isotropic phase ($S \simeq 0.072$); whereas, at the higher pressure $P = 1.745$, one has already entered the nematic regime ($S \simeq 0.343$). For $N = 10\,000$, the IN phase transition is already relatively sharp as these numbers indicate. Whereas this already suggests that, in the limit $N \to \infty$, one is probably dealing with a discontinuous rather than a continuous phase transition, plots in Fig. 7(b) provide further evidence for this interpretation. These plots reveal that, over a relatively large range of intermolecular separations r, $G_2^c(r)$ can be described by an exponential function as discussed at the end of Sec. III B. A fit of an exponential function gives $\ell \simeq 2.13$ at $P = 1.735$, whereas an only slightly larger value of $\ell \simeq 2.33$ is observed at $P = 1.745$ immediately above the IN phase transition. In other words, across the IN phase transition, ℓ does not exceed two times the length of the long molecular axis. Moreover, directly at the IN phase transition, ℓ remains smaller by a factor of 3 than the length of the computational cell for the smallest system studied ($N = 300$, $L \simeq 7$). From our data, it seems unlikely to expect that $\ell \to \infty$ as one would if the IN phase transition were continuous. Similar observations have been made by Weber who found that ℓ passes through a maximum at the IN phase transition but remains small and finite [66].

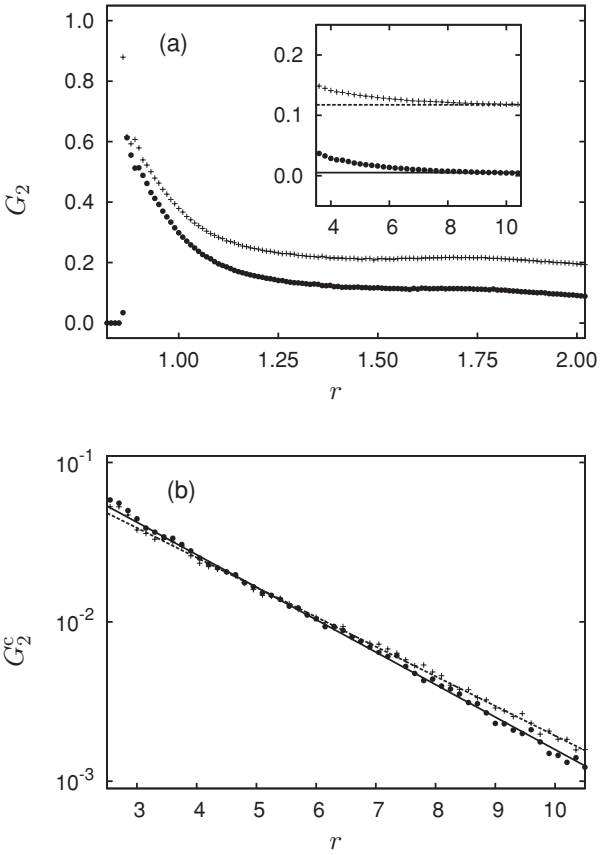

FIG. 7. (a) Orientational correlation function $G_2(r)$ for $N = 10\,000$ and ●, $P \simeq 1.735$ and +, $P \simeq 1.745$. The inset shows long-range behavior of $G_2(r) \to S^2$ [—, $S \simeq 0.072$ and - - - -, $S \simeq 0.343$, see Eq. (3.13)]. (b) as (a) but for $G_2^c(r)$ on a semilogarithmic scale; lines are fits of an exponential function to the curves for —, $P \simeq 1.735$ and - - - -, $P \simeq 1.745$.

E. Predictions of Landau theory

Finally, it seems worthwhile to analyze the IN phase transition in terms of Landau's theory of phase transitions [50]. To that end, one expresses the relevant thermodynamic potential as a Taylor series in terms of the order parameter. In the present case, where the relevant thermodynamic field driving the phase transition is the pressure, we may expand $\mathcal{G}$ in terms of $\mathbf{Q}$ as [50]

$$\beta\mathcal{G} = \beta\mathcal{G}_0 + \tfrac{1}{2}A(P)\langle\mathbf{Q}\rangle : \langle\mathbf{Q}\rangle + \tfrac{1}{3}B(P)\langle\mathbf{Q}\rangle : (\langle\mathbf{Q}\rangle \cdot \langle\mathbf{Q}\rangle) + \tfrac{1}{4}C(P)(\langle\mathbf{Q}\rangle : \langle\mathbf{Q}\rangle)^2 + \cdots, \quad (4.5)$$

where $A(P)$, $B(P)$, and $C(P)$ are dimensionless coefficients depending only on P under the present isothermal conditions. In Eq. (4.5), we employ the notation of Gray and Gubbins for single and double contractions of the second-rank tensor $\mathbf{Q}$ [44]. In the uniaxial case ($\xi = 0$) and after diagonalizing $\mathbf{Q}$ in the basis of its eigenvectors, it follows from Eq. (3.8) that second- and third-order scalar invariants of $\mathbf{Q}$ are given by

$$\langle\mathbf{Q}\rangle : \langle\mathbf{Q}\rangle = \tfrac{3}{2}S^2, \quad (4.6a)$$

$$\langle\mathbf{Q}\rangle : (\langle\mathbf{Q}\rangle \cdot \langle\mathbf{Q}\rangle) = \tfrac{3}{4}S^3, \quad (4.6b)$$

and, therefore, [50],

$$\beta\mathcal{G} = \beta\mathcal{G}_0 + \tfrac{3}{4}A(P)S^2 + \tfrac{1}{4}B(P)S^3 + \tfrac{9}{16}C(P)S^4 + \cdots. \tag{4.7}$$

Notice that the expansion of $\beta\mathcal{G}$ starts with the second-order scalar invariant of $\mathbf{Q}$ as the first nontrivial term because the first-order scalar invariant $\mathrm{Tr}\,\mathbf{Q} = 0$ on account of Eq. (3.7). In principle, $A(P)$, $B(P)$, and $C(P)$ may be obtained from $\mathcal{P}(S)$ because [54]

$$\mathcal{P}(S) = \mathcal{P}_0 \exp\left[-\beta\mathcal{G}(S)\right], \tag{4.8}$$

where the normalization constant $\mathcal{P}_0$ is determined such that

$$\int_0^1 dS\mathcal{P}(S) = 1 \tag{4.9}$$

according to the discussion in Sec. 5.6.3 of Chap. 1 in Ref. [11].

In the simulations, we obtain $\mathcal{P}(S)$ as a histogram using a width $\delta S = 0.005$ for the histogram bins. Plots in Fig. 8 reveal that, in the isotropic phase and sufficiently far away from the IN phase transition, $\mathcal{P}(S)$ exhibits a single maximum. This maximum is larger the smaller P is. Likewise, the width of $\mathcal{P}(S)$ increases as P increases toward P^*. In the immediate vicinity of the IN phase transition, $\mathcal{P}(S)$ becomes bimodal where the two peaks of the distribution are not completely separated because our system is still finite. However, we notice that the shape of this bimodal distribution can still be fitted very well with the Landau expansion of $\beta\mathcal{G}$. In a sequence of very careful simulations, we have also been able to determine $\mathcal{P}(S)$ directly at the pressure $P^* \simeq 1.74$ at which the cumulants g_2^0 and g_2^+ apparently intersect (see Fig. 4). It is particularly gratifying that, at this pressure, $\mathcal{P}(S)$ is bimodal with two peaks of equal height as the inset in Fig. 8 clearly shows. Hence, in the sense of Eq. (4.8), $\mathcal{P}(S)$ at P^* may be interpreted as an order-parameter distribution for coexisting isotropic and nematic phases in a system of finite size.

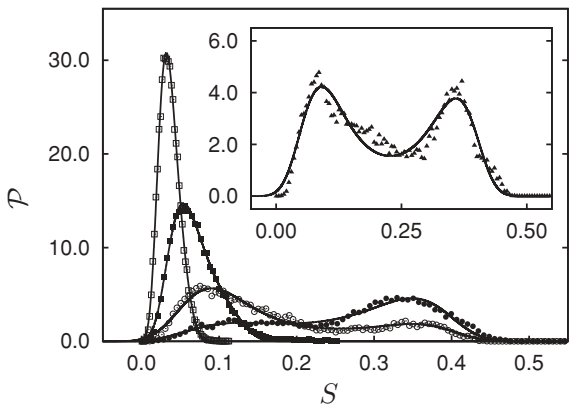

FIG. 8. Order-parameter distribution $\mathcal{P}(S)$ as a function of the nematic-order parameter S for $N = 5000$; □, $P = 1.00$; ■, $P = 1.60$; ○, $P = 1.70$; and ●, $P = 1.75$. Full line is a fit based upon $\mathcal{G}$ from Eq. (4.7) treating $A(P)$, $B(P)$, and $C(P)$ as fit parameters and replacing $S \to S - S_{\mathrm{res}}$ where the residual nematic-order parameter S_{res} is treated as an additional fit parameter accounting for the nonvanishing nematic order in any finite system [see Fig. 2(a)]. The inset shows $\mathcal{P}(S)$ directly at ▲, $P^* \simeq 1.74$ (see also Fig. 4).

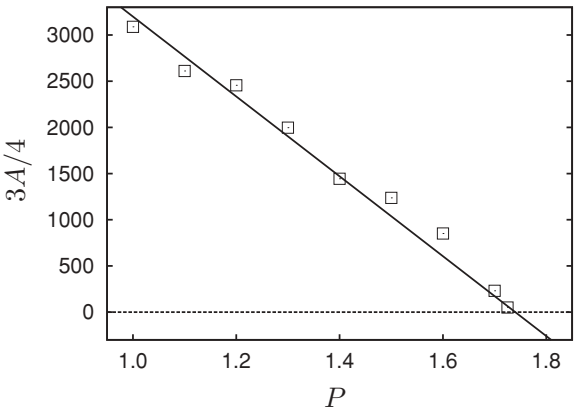

FIG. 9. Plot of $A(P)$ in the Landau expansion of $\beta\mathcal{G}$ [see Eq. (4.7)] as a function of pressure □, P. The solid line is a fit of Eq. (4.10) to the discrete data points taking A_0 as a fit parameter and $P^* = 1.74$ from the cumulant analysis presented in Sec. IV C.

It is also apparent from the plots in Fig. 8 that $\mathcal{P}(S)$ is not Gaussian in agreement with the Landau expansion of $\mathcal{G}$ in Eq. (4.7) if one assumes both $B(P)$ and $C(P)$ to be appreciable in magnitude. We obtain information about $A(P)$, $B(P)$, and $C(P)$ by fitting Eqs. (4.7) and (4.8) to the histograms representing $\mathcal{P}(S)$. As noted earlier by Eppenga and Frenkel [54], $B(P)$ and $C(P)$ are determined mostly by the wings of $\mathcal{P}(S)$, which can only be determined with limited accuracy so that we refrain from plotting any data. However, our results seem to suggest that $B(P)$ decreases toward P^* but remains small, whereas, $C(P) > 0$ everywhere. These general features are consistent with requirements of Landau's theory as far as discontinuous phase transitions are concerned (see Sec. 143 of Ref. [46]). At such a transition, $A(P)$ has to change sign at P^*. Here, the usual assumption [46] is that, sufficiently close to P^*,

$$A(P) = A_0(P - P^*), \tag{4.10}$$

such that $A(P)$ changes sign at $P = P^*$. Results of our fit plotted in Fig. 9 are consistent with this general prediction of Landau's theory, thereby supporting our earlier conclusion that the IN phase transition in the Hess-Su model is likely to be weakly discontinuous.

V. DISCUSSION AND CONCLUSIONS

In this paper, we employed Monte Carlo simulations in the isothermal-isobaric ensemble to investigate finite-size effects at the IN phase transition in the Hess-Su model of a liquid crystal [35] and to gain a more detailed picture of the nature of this phase transition. In particular, we wished to determine whether this phase transition was continuous or discontinuous. Finite-size effects manifest themselves most directly as nonvanishing values of the nematic-order parameter S in the isotropic phase. From an operational point of view, S is usually computed as an ensemble average of a suitably chosen eigenvalue of the alignment tensor $\mathbf{Q}$. From the pioneering work by Eppenga and Frenkel, one knows how these ensemble averages should scale with the number of molecules N both in the isotropic and in the nematic phases and, of course,

irrespective of the specific model system [54]. Later, Weber *et al.* proposed similar scaling laws for higher-order moments of the eigenvalue distributions [34]. All these scaling laws are confirmed numerically in this paper and for the range of system sizes chosen.

Another fingerprint of finite-size effects is an ostensible biaxiality ξ that is small but does not vanish completely, although the molecules of our model are uniaxial and there are no external fields that would cause nematic phases to have true biaxial symmetry [39]. From the scaling relations for ensemble averages of eigenvalues of $\mathbf{Q}$, the system-size dependence of ξ is given by $N^{-1/2}$ both in the isotropic and in the nematic phases. Here, this prediction is tested and is confirmed, at least, for sufficiently large system sizes. The detailed investigation of various scaling predictions is important because it allows us to verify that the range of system sizes chosen for this paper is large enough for our model. Moreover, the confirmation of analytically predicted scaling laws indicates that the statistical accuracy of our Monte Carlo results is sufficient to determine both location P^* and nature of the IN phase transition in the Hess-Su model.

In this regard, the cumulant intersection method originally proposed by Binder [4,5] is particularly useful. Based upon the second-order cumulant of λ_+ and λ_0 of $\mathbf{Q}$, we obtain $P^* = 1.74$ at the given temperature $T = 1.00$. In this regard, it is somewhat striking that our cumulants seem to intersect at a universal pressure P^* irrespective of system size and seemingly contrary to what one would have anticipated for a discontinuous phase transition. However, following arguments put forth by Vollmayr *et al.* [20], this observation alone is insufficient to conclude that the IN phase transition is, in fact, continuous. In principle, it is conceivable that, at a very weak discontinuous phase transition, one may fail to observe the anticipated shift of the intersection between pairs of cumulants proportional to N^{-1}. This could happen if, for instance, the constant of proportionality is too small to be detected given the statistical accuracy of the data. In fact, looking at Fig. 8 of Ref. [34], one sees that their system-size-dependent temperature $T_{\mathrm{cr}}(L)$ changes rather weakly with L for lattices with more than only $L = 10$ sites.

Therefore, to decide whether the IN phase transition in the present model is continuous or discontinuous, additional information is required. To that end, we compute the orientation correlation function $G_2(r)$ for a large system with $N = 10\,000$ molecules. Around the phase transition, $G_2^{\mathrm{c}}(r)$ exhibits an exponential decay governed by a correlation length ℓ, which does not exceed twice the long axis of our molecules and, thus, remains finite and small in the immediate vicinity of the IN phase transition. Similar observations have been made earlier by Weber for his lattice model of flexible polymer chains. For example, in his thesis, Weber shows that ℓ remains finite but passes through a weak maximum during the IN phase transition [66]. The finiteness of ℓ clearly points to a discontinuous phase transition. However, if that were the case, one anticipates the maximum of the associated isobaric heat capacity to scale proportional to N. In the actual simulations, we find an increase of $c_{\mathrm{P}}^{\mathrm{m}} \propto N^y$ where $y \simeq 0.58$ is significantly *smaller* than 1. On the other hand, y is significantly *larger* than $\frac{2}{3\nu} - 1 \simeq 0.06$ expected for a continuous phase transition [20]. The scaling of $c_{\mathrm{P}}^{\mathrm{m}}$, with an effective exponent intermediate to that characteristic of a continuous and that of a discontinuous phase transition, parallels results obtained by Vollmayr *et al.* for a thermally driven discontinuous phase transition in a three-dimensional q-state Potts model ($q \geqslant 3$). Moreover, we notice that, for particle numbers $500 \leqslant N \leqslant 5000$, the shift of $c_{\mathrm{P}}^{\mathrm{m}}$ with N is surprisingly minute. This seems consistent with the observation that we have been unable to detect any dependence of the intersection between pairs of neighboring cumulants g_2^0 and g_2^+ with N.

The apparent insensitivity of the location of $c_{\mathrm{P}}^{\mathrm{m}}$ to changes in N is particularly gratifying in view of our earlier studies of the IN phase transition in various confined geometries [38,39]. In these works, we located the IN phase transition solely via the position of the maximum of the isobaric heat capacity and only for $1500 \leqslant N \leqslant 2000$ molecules. From our present more extensive investigation, we conclude that, in this range of particle numbers, $c_{\mathrm{P}}^{\mathrm{m}}$ is a sufficiently accurate indicator to locate the IN phase transition. Nevertheless, it needs to be stressed that the value of $P^* \simeq 1.70$ first reported by Steuer *et al.* [37] and confirmed later by us [38], which was based upon system sizes of $N = 1000$ [37] and $N = 1500$ [38], is presumably a bit too low because of a small residual system-size effect.

Moreover, it is interesting to note that Landau's theory of phase transitions [46] seems qualitatively applicable here similar to what has been concluded by Eppenga and Frenkel [54] for their model liquid crystal of hard platelets. Within this theory, the continuous or discontinuous character of a phase transition depends on whether or not the coefficient B in front of the third-order term of the expansion of the thermodynamic potential vanishes [46,50]. Although our data do not permit us to distinguish, with absolute certainty, between the two, they seem to suggest that B is small but nonzero at P^*. In addition, at the IN phase transition, the symmetric bimodal shape of $\mathcal{P}(S)$ reveals that the free-energy barrier $\beta\Delta\mathcal{G}$ separating coexisting isotropic and nematic states (see, for example, the inset in Fig. 8) is only on the order of $k_B T$. Therefore, the IN phase transition is most likely to be weakly discontinuous. This notion is corroborated further by the observation that the variation of S with P still looks rather smooth even for $N = 5000$. Moreover, the pronounced peak in plots of c_{P} versus P indicates a loss of orientational entropy caused by the preferential alignment of molecules with the director $\hat{\boldsymbol{n}}$ as one goes from the isotropic to the nematic phase [38]. Thus, we conclude that all observations made in this paper are consistent with a weakly discontinuous entropy-driven IN phase transition. Similar conclusions have been reached for the lattice polymer model investigated by Weber *et al.* [34] despite the fact that, in their study, the IN phase transition was thermally driven.

ACKNOWLEDGMENTS

We are grateful to Professor Kurt Binder (Johannes-Gutenberg Universität Mainz) and Dr. Pawel Bryk (Uniwersytet Marii-Curie Skłodowskiej) for reading our manuscript and commenting, in detail, on our results. In addition, we are most grateful to an anonymous referee for bringing

Refs. [64,65] to our attention and for very insightful and helpful comments that doubtlessly led to a substantial improvement of our presentation. We are also grateful for financial support from the International Graduate Research Training Group 1524 "Self-assembled soft-matter nanostructures at interfaces."

[1] T. L. Hill, *Thermodynamics of Small Systems* (Dover, Mineola, NY, 2002).
[2] Y. Imry, Phys. Rev. B **21**, 2042 (1980).
[3] D. P. Landau and K. Binder, *A Guide to Monte Carlo Simulations in Statistical Physics*, 2nd ed. (Cambridge University Press, Cambridge, UK, 2005).
[4] K. Binder, Z. Phys. B: Condens. Matter **43**, 119 (1981).
[5] K. Binder, Phys. Rev. Lett. **47**, 693 (1981).
[6] K. Wilson, Phys. Rev. B **4**, 3174 (1971).
[7] K. Wilson, Phys. Rev. B **4**, 3184 (1971).
[8] M. Gell-Mann and F. E. Low, Phys. Rev. **95**, 1300 (1954).
[9] K. Binder, Ann. Rev. Phys. Chem. **43**, 33 (1992).
[10] K. Binder, *Computational Methods in Field Theory* (Springer-Verlag, Berlin, 1992), p. 57.
[11] V. Privman, *Finite Size Scaling and Numerical Simulation of Statistical Systems* (World Scientific, Singapore, 1990).
[12] K. Binder and D. W. Heermann, *Monte Carlo Simulation in Statistical Physics* (Springer-Verlag, Berlin, 1988).
[13] J. L. Cardy, *Finite Size Scaling* (North-Holland, Amsterdam, 1988).
[14] K. Binder, Ferroelectrics **73**, 43 (1987).
[15] M. N. Barber, *Phase Transitions and Critical Phenomena* (Academic, New York, 1983), p. 145.
[16] H. E. Stanley, *Phase Transitions and Critical Phenomena* (Oxford University Press, Oxford, 1971).
[17] M. E. Fisher, in *Critical Phenomena*, Proceedings of the 1970 Enrico Fermi International School of Physics (Academic, New York, 1971), p. 1.
[18] K. Binder and D. P. Landau, Phys. Rev. B **30**, 1477 (1984).
[19] M. S. S. Challa, D. P. Landau, and K. Binder, Phys. Rev. B **34**, 1841 (1986).
[20] K. Vollmayr, J. D. Reger, M. Scheucher, and K. Binder, Z. Phys. B: Condens. Matter **91**, 113 (1993).
[21] R. L. C. Vink, Phys. Rev. Lett. **98**, 217801 (2007).
[22] M. Rovere, D. W. Heermann, and K. Binder, J. Phys. Condens. Matter **2**, 7009 (1990).
[23] A. D. Bruce and N. B. Wilding, Phys. Rev. Lett. **68**, 193 (1992).
[24] N. B. Wilding, Phys. Rev. E **52**, 602 (1995).
[25] J. J. Potoff and A. Z. Panagiotopoulos, J. Chem. Phys. **109**, 10914 (1998).
[26] J.-H. Wang and Y.-L. Ma, J. Phys. B **43**, 175301 (2010).
[27] E. Mondal and S. K. Roy, Phys. Lett. A **312**, 397 (2003).
[28] D. Jayasri, V. S. S. Sastry, and K. P. N. Murthy, Phys. Rev. E **72**, 036702 (2005).
[29] J. M. Fish and R. L. C. Vink, Phys. Rev. B **80**, 014107 (2009).
[30] J. M. Fish and R. L. C. Vink, Phys. Rev. E **81**, 021705 (2010).
[31] N. G. Almarza, C. Martín, and E. Lomba, Phys. Rev. E **80**, 031501 (2009).
[32] L. G. López, D. H. Linares, and A. J. Ramirez-Pastor, Phys. Rev. E **80**, 040105 (2009).
[33] R. L. C. Vink and T. Schilling, Phys. Rev. E **71**, 051716 (2005).
[34] H. Weber, W. Paul, and K. Binder, Phys. Rev. E **59**, 2168 (1999).
[35] S. Hess and B. Su, Z. Naturforsch. **54a**, 559 (1999).
[36] H. Steuer, S. Hess, and M. Schoen, Physica A **328**, 322 (2003).
[37] H. Steuer, S. Hess, and M. Schoen, Phys. Rev. E **69**, 031708 (2004).
[38] M. Greschek, M. Melle, and M. Schoen, Soft Matter **6**, 1898 (2010).
[39] M. Greschek and M. Schoen, Soft Matter **6**, 4931 (2010).
[40] D. Frenkel and R. Eppenga, Phys. Rev. A **31**, 1776 (1985).
[41] H. Kunz and G. Zumbach, Phys. Rev. B **46**, 662 (1992).
[42] M. A. Bates and D. Frenkel, J. Chem. Phys. **112**, 10034 (2010).
[43] D. A. McQuarrie, *Statistical Mechanics* (Harper & Row, New York, 1976).
[44] C. G. Gray and K. E. Gubbins, *Theory of Molecular Fluids* (Clarendon, Oxford, 1984), Vol. 1.
[45] T. Gruhn and M. Schoen, Phys. Rev. E **55**, 2861 (1997).
[46] L. D. Landau and E. M. Lifschitz, *Lehrbuch der Theoretischen Physik* (Akademie Verlag, Berlin, 1987), Vol. V.
[47] W. Maier and A. Saupe, Z. Naturforsch. A **14**, 882 (1959).
[48] W. Maier and A. Saupe, Z. Naturforsch. A **15**, 287 (1960).
[49] G. Vertogen and W. H. de Jeu, *Thermotropic Liquid Crystals, Fundamentals* (Springer-Verlag, Berlin, 1988).
[50] P. G. de Gennes and J. Prost, *The Physics of Liquid Crystals* (Clarendon, Oxford, 1995).
[51] I. Pardowitz and S. Hess, Physica A **100**, 540 (1980).
[52] W. H. Press, S. A. Teukolsky, W. T. Vetterling, and B. P. Flannery, *Numerical Recipes in FORTRAN* (Cambridge University Press, Cambridge, UK, 1989).
[53] A. Richter and T. Gruhn, J. Chem. Phys. **125**, 064908 (2006).
[54] R. Eppenga and D. Frenkel, Mol. Phys. **52**, 1303 (1984).
[55] G. Arfken, *Mathematical Methods for Physicists* (Academic, San Diego, 1985).
[56] R. Low, Eur. J. Phys. **23**, 111 (2002).
[57] C. Zannoni, *The Molecular Physics of Liquid Crystals* (Academic, London, 1979), Chap. 3, p. 76.
[58] R. V. Gavai, F. Karsch, and B. Peterson, Nucl. Phys. B **322**, 738 (1989).
[59] M. Schoen, Physica A **270**, 353 (1999).
[60] M. Allen and D. Tildesley, *Computer Simulation of Liquids* (Oxford Science Publications, Oxford, 1986).
[61] N. B. Wilding and K. Binder, Physica A **231**, 439 (1996).
[62] M. G. Mazza, M. Greschek, R. Valiullin, J. Kärger, and M. Schoen, Phys. Rev. Lett. **105**, 227802 (2010).
[63] A. M. Ferrenberg and D. P. Landau, Phys. Rev. B **44**, 5081 (1991).
[64] A. D. Bruce and N. B. Wilding, Phys. Rev. E **60**, 3748 (1999).
[65] L. A. Fernandez, A. Gordillo-Guerrero, V. Martin-Mayor, and J. J. Ruiz-Lorenzo, Phys. Rev. E **80**, 051105 (2009).
[66] H. Weber, Ph.D. thesis, Johannes-Gutenberg Universität Mainz, 1997 (unpublished).